Combinatorial CRISPR screen reveals *FYN* and *KDM4* as targets for synergistic drug combination for treating triple negative breast cancer

Running title: FYN and KDM4 inhibition synergizes with TKIs

Tackhoon Kim[1,2,3,4,*] Byung-Sun Park[1,2], Soobeen Heo[5], Heeju Jeon[1,2], Jaeyeal Kim[1,2], Donghwa Kim[6], Sang Kook Lee[6], So-Youn Jung[7], Sun-Young Kong[5,8], Timothy K. Lu[4,*]

[1] Medicinal Materials Research Center, Korea Institute of Science and Technology, 5 Hwarangro-14-gil, SeongbukGu, Seoul 02792, Republic of Korea

[2] Department of Biological Sciences, Korea University, 145 AnamRo, SeongbukGu, Seoul 02841, Republic of Korea

[3] Division of Bio-Medical Science and Technology, Korea University of Science and Technology, 217 GajeongRo, YuseongGu, Daejeon 34113, Republic of Korea

[4] Research Lab of Electronics, Massachusetts Institute of Technology, 77 Massachusetts Avenue, Cambridge MA 02139, USA

[5] Targeted Therapy Branch, Division of Rare and Refractory Cancer, Research Institute, National Cancer Center, Goyang 10408, Korea

[6] College of Pharmacy, Natural Products Research Institute, Seoul National University, 1 Gwanakro, Gwanakgu, Seoul 08826, Republic of Korea.

[7] Division of Breast Surgery, Department of Surgery, National Cancer Center, Goyang 10408, Korea

[8] Department of Laboratory Medicine, National Cancer Center, Goyang 10408, Republic of Korea

* **Correspondence**: Tackhoon Kim, 5 Hwarangro-14-gil, SeongbukGu, Seoul 02792, Republic of Korea;

Timothy K. Lu, 500 Technology Square, Cambridge MA 02139, USA.

Email: tackhoon@kist.re.kr; tim@lugroup.org

Competing Interest Statement

The authors declare no conflict of interest

Abstract

Tyrosine kinases play a crucial role in cell proliferation and survival and are extensively investigated as targets for cancer treatment. However, the efficacy of most tyrosine kinase inhibitors (TKIs) in cancer therapy is limited due to resistance. In this study, we identify a synergistic combination therapy involving TKIs for the treatment of triple negative breast cancer. By employing pairwise tyrosine kinase knockout CRISPR screens, we identify *FYN* and *KDM4* as critical targets whose inhibition enhances the effectiveness of TKIs, such as NVP-ADW742 (IGF-1R inhibitor), gefitinib (EGFR inhibitor), and imatinib (ABL inhibitor) both *in vitro* and *in vivo*. Mechanistically, treatment with TKIs upregulates the transcription of *KDM4*, which in turn demethylates H3K9me3 at *FYN* enhancer for *FYN* transcription. This compensatory activation of *FYN* and *KDM4* contributes to the resistance against TKIs. *FYN* expression is associated with therapy resistance and persistence by demonstrating its upregulation in various experimental models of drug-tolerant persisters and residual disease following targeted therapy, chemotherapy, and radiotherapy. Collectively, our study provides novel targets and mechanistic insights that can guide the development of effective combinatorial targeted therapies, thus maximizing the therapeutic benefits of TKIs.

Introduction

Tyrosine kinases have emerged as important drug targets in cancer therapy due to their druggability and pivotal roles in cell proliferation and survival(1). They are implicated in various aspects of cancer development(2), such as cell survival, proliferation, angiogenesis, and invasion, making them attractive targets for drug intervention. Consequently, tyrosine kinase inhibitors (TKIs) have gained considerable attention as primary agents for cancer treatment.

Triple negative breast cancer (TNBC) treatment has limited options for targeted therapy. TNBC, characterized by the absence of estrogen receptor, progesterone receptor, and HER2 expression, exhibits elevated activity of tyrosine kinases, including EGFR and IGF1R(3, 4). However, several clinical trials investigating TKIs, such as VEGFR inhibitors, EGFR inhibitors, and FGFR inhibitors, in TNBC treatment have yielded disappointing results due to inadequate efficacy. Therefore, it is crucial to comprehend the mechanisms underlying TNBC's suboptimal response to TKIs to enable the development of more effective targeted therapies against TNBC.

The therapeutic efficacy of TKIs is compromised by intrinsic and acquired resistance(5). For instance, EGFR inhibitor gefitinib extended the median progression-free survival by only five months compared to conventional

53 chemotherapy in non-small cell lung cancer (NSCLC) patients with EGFR mutation(6). Significant subset of
54 drug resistance is driven by gene interactions that enable compensatory changes in signal transduction upon
55 drug treatment. Compensatory activation of mitogenic signals, such as MET, PIK3CA amplification, and
56 MAPK/ERK signaling activation, counterbalances the inhibition of EGFR by TKI osimertinib in a significant
57 portion of NSCLC patients(7). Simultaneous inhibition of multiple signaling molecules that compensate for
58 each other's loss is proposed as an effective strategy to overcome resistance to kinase inhibitor therapy,
59 emphasizing the importance of combinatorial therapy(8).

60 Until recently, a highly scalable method for screening combinatorial therapy has been lacking. Combinatorial
61 CRISPR screens have emerged as efficient tools to identify synergistic targets for combinatorial therapy. We and
62 others recently developed combinatorial CRISPR screens to elucidate pairwise gene interactions(9-12). Our
63 combinatorial genetic screen platform, combinatorial genetics *en Masse* (combiGEM), was successfully
64 implemented to identify combinations of epigenetic regulators causing synthetic lethality in ovarian cancer cells
65 (9).

66 In this study, we utilize CombiGEM-CRISPR technology to identify tyrosine kinase inhibitor combinations with
67 synergistic effect in TNBC cell line and xenograft models for potential combinatorial therapy against TNBC.
68 We highlight FYN as a key therapeutic target that, when inhibited, enhances the cytotoxic effect of inhibition of
69 other tyrosine kinases (IGF1R, EGFR, and ABL2). Mechanistic studies reveal KDM4 as a crucial epigenetic
70 regulator that demethylates H3K9me3 and transcriptionally upregulates *FYN* upon TKI treatment. *In vitro* and *in*
71 *vivo* validation demonstrates the synergistic TNBC-shrinking effects of combining PP2, saracatinib (Src family
72 kinase / FYN inhibitor) or QC6352 (KDM4 inhibitor) with TKIs. Additionally, we demonstrate the clinical
73 significance of our findings by observing upregulation of *FYN* in various models of drug tolerant persisters and
74 residual tumors after chemo-, radio-, or targeted therapy. Therefore, simultaneous targeting of *FYN-KDM4* and
75 tyrosine kinase pathways through combinatorial therapy holds promise for effective therapy against TNBC.

76

77 **Results**

78 **Pairwise tyrosine kinase knockout CRISPR screen reveals synergistic tyrosine kinase inhibition**
79 **combination**

For efficient translation of CRISPR screening data to drug combination, we selected 76 tyrosine kinases that could be inhibited by at least one drug from the drug repurposing hub database (table S1) (13). For pairwise CombiGEM library construction, we chose three guide RNAs from the optimized Brunello single guide RNA (sgRNA) list(14) employing the iterative cloning method as previously described(9, 15). The resulting library enabled screens of pairwise knockouts of the 76 tyrosine kinase genes, encompassing 54,289 sgRNA pairs representing 3,003 pairwise gene disruptions (Fig. 1A). To validate our library, we performed next-generation sequencing and confirmed that 99.5% (2,989/3,003) of gene pairs were represented by at least 6 pairs of sgRNAs, with the $\log_{10}$ reads per million of 0.5 (Fig. S1A).

Triple negative breast cancer cell line MDA-MB-231 cells stably expressing Cas9 were transduced with the lentiviral library at low multiplicity of infection (MOI) of 0.3. Genomic DNA was harvested 3 days after transduction (designated as day 0[D0]), and 23 days after transduction (D20) (Fig. 1A) to perform PCR amplification of sgRNA pairs for subsequent next-generation sequencing (NGS) analysis. sgRNAs, instead of barcodes in our previous CombiGEM screens, were directly sequenced using paired-end sequencing to rule out uncoupling of barcodes of sgRNAs and barcodes (Fig. S1B-C). We counted the occurrences of each sgRNA pair in the NGS data and calculated the normalized log2 fold change in counts between the day 20 and day 0 samples as the growth phenotype score Z (see Methods). The Z scores for the two permutations of an sgRNA pair (r=0.50 between sgRNA-A + sgRNA-B and sgRNA-B + sgRNA-A pairs), the biological replicates, (r = 0.74 between replicates #2 and #3), and independent sgRNA pairs targeting the same set of genes were positively correlated (r=0.3-0.72) (Fig. S1D-G).

Gene pairs that synergistically kill cells were identified by calculating gene interaction scores (GI). The GI scores were derived by comparing the growth phenotype score Z resulting from the disruption of a gene pair (Z_{A+B}, observed Z score) to the sum of Z scores obtained from the disruption of each gene individually within the pair ($Z_{A+Con} + Z_{B+Con}$, expected Z score) (Fig. 1B). The expected and observed Z scores for each gene (or sgRNA) pair exhibited a strong positive correlation (r=0.97 gene level, r=0.88 sgRNA level), suggesting that most random pairwise combinations of tyrosine kinase perturbations show additive effects (Fig. 1B and S1H). GI scores were calculated by quantifying each gene pair's normalized deviation from the quadratic fit of the expected-observed Z score plot(10) (Fig.1C and Fig. S1I, see methods).

We selected thirty synthetic lethal gene pairs using cutoffs for gene level GI score <-2 and p<0.01 for GI scores

108 determined by RIGER analysis(16) and Z<-5 (Fig. 1D and dataset S1). Among these, the SRC-YES pair was
109 one of the strongest synthetic lethal gene pairings (GI= -3.95). Notably, SRC-YES belong to the same tyrosine
110 kinase family and are known to be functionally redundant and are expected to be synthetic lethal(17). These
111 findings provide evidence for the effectiveness of our screening approach in identifying synthetic lethal gene
112 pairs.

113 Synthetic lethal gene pairs are next validated by expressing the pair of sgRNAs targeting them. To achieve this,
114 we introduced lentiviral vectors carrying two distinct sgRNAs targeting the candidate synthetic lethal pairs, each
115 tagged with a different fluorescent protein (GFP and mCherry). MDA-MB-231 Cas9 cells were transduced with
116 the lentivirus at a low titer (MOI ~0.5), resulting in a mixed population of cells expressing either one or both
117 sgRNAs along with their respective fluorescent proteins (Figs. 2A and S2A). We monitored the decrease in the
118 number of GFP/mCherry double-positive cells to evludate synthetic lethality (see methods). We validated the
119 efficacy of the sgRNAs used in Figure 2A through the T7 endonuclease assay, which confirmed efficient gene
120 editing (Fig. S2B). Consistent with our CRISPR screening results, we observed that the disruption of six out of
121 eight synergistic target gene combinations led to a reduction in cell viability beyond what was predicted by the
122 Bliss independence model (Fig. 2B). Moreover, the relative viability of double knockout cells and the rate of
123 synergistic killing demonstrated a strong correlation with our screening data (r = 0.65 for both viability and
124 synergistic effect; Fig. S2C). Collectively, our findings provide compelling evidence that our screening approach
125 successfully identified synthetic lethal gene pairs with a high level of confidence.

126 **FYN inhibition synergizes with IGF1R, EGFR, ABL2 inhibitions in cell killing**

127 We noticed that several validated synergistic target gene pairs included *FYN* (e.g. *FYN*+IGF1R, *FYN*+EGFR,
128 and *FYN*+ABL2). Notably, network analysis of the 30 candidate synergistic tyrosine kinase pairs revealed that
129 *FYN* is one of the key nodes participating in synergistic interactions with multiple genes (Fig. 2C). Expression
130 of FYN, a member of Src family kinase, has been implicated in cancer malignancy including drug resistance(18-
131 21). Particularly, recent studies highlighted significant contribution of FYN in TNBC malignancy by promoting
132 epithelial-to-mesenchymal transition (EMT)(22, 23). Interestingly, we found that *FYN*, but not *SRC*, exhibited
133 significant upregulation in triple-negative breast cancer (TNBC) compared to other subtypes, as evidenced by
134 microarray data from primary tumor samples (24) and the cancer cell line encyclopedia (CCLE)(25) (Figs. 2D-
135 E). In contrast, other key nodes in figure 2C, including FGFR2, FRK and TEK were not expressed at

136 appreciable levels in MDA-MB-231 (log2(TPM+1) for TEK: 0.0704, FRK:0.124, FGFR2:0.227), and their
137 expressions were not significantly upregulated in TNBCs compared to other breast cancer subtypes (Fig. S3).
138 Therefore, we proceeded further in focusing on validating FYN as key candidate synthetic lethal gene. These
139 findings suggest that FYN could represent an attractive drug target for TNBC treatment. To investigate this
140 further, we assessed whether simultaneous inhibition of FYN by PP2, which selectively targets the SRC family
141 kinase inhibitor with the highest potency against FYN, in combination with other kinase inhibitors (TKIs), could
142 inhibit cancer cell growth(26). PP2 as a single agent significantly downregulated MDA-MB-231 cell viability
143 (Fig. S4A). Therefore, we focused on synergistic cell death by TKI combinations above additive effects by each
144 TKI. To this end, analysis using SynergyFinder plus(27)revealed that all TKI combinations involving PP2 and
145 NVP-ADW742 (IGF1R inhibitor), gefitinib (EGFR inhibitor) or imatinib (ABL inhibitor) synergistically
146 induced cell death in MDA-MB-231 cells (Fig. 2F). Dose-response curves demonstrated that co-treatment with
147 PP2 reduced the IC50 of the tested TKIs by 34-61%, indicating that PP2 sensitized cancer cells to TKI treatment
148 (Fig. 2G). Similar synergy was observed when TKI combinations included saracatinib, a SRC family kinase
149 inhibitor(28), in place of PP2 (Fig. S4B). Moreover, specific ablation of *FYN*, but not *SRC*, sensitized cells to
150 TKIs, highlighting the critical role of FYN as a member of SRC kinase family responsible for TKI resistance
151 (Figs. 2H and S4C). Ablation of FYN itself did not significantly decrease cell viability (Fig. S4D). Importantly,
152 we observed similar synergy between the same drug combinations in other TNBC cell lines, including Hs578T,
153 HCC1143, HCC1395, and HCC1937 cells (Figs. S4E-H). Further assessment using live-dead and BrdU assays
154 revealed that both the PP2+NVP-ADW742 and PP2+gefitinib combinations synergistically induced cell death
155 while inhibiting cell growth (Fig. 2I).

156 Persistent activation of MAPK pathway and PI3K-AKT pathway has been associated with TKI resistance in
157 various cancers(5). Therefore, we investigated which downstream pathways were involved in sensitizing cells to
158 TKI treatment. Notably, the p38 MAPK was significantly attenuated following treatment with either PP2 or
159 saracatinib treatment (Fig. 2J). Previous studies with imatinib resistant CML cells identified ERK signaling as
160 critical downstream of FYN activation(19, 20). However, FYN inhibition failed to significantly downregulate
161 phosphorylated ERK level upon imatinib treatment, indicating downstream signals of FYN leading to drug
162 resistance may be context dependent. Genetic ablation of *FYN* similarly reduced p38 activation (Fig. 2K).
163 Attenuation of p38 activity was also observed in an independent TNBC cell line, Hs578T (Figs. S4I-J).
164 Importantly, treatment of p38 MAPK pathway inhibitor SB203580 markedly sensitized cells to TKI treatment

165 (Fig. 2L), while SB203580 as single agent did not significantly change cell viability (Fig. S4K)

166 **FYN mRNA is induced upon TKI treatment in KDM4 dependent manner**

167 Our discovery that inhibition of FYN synergizes with multiple TKIs possessing distinct target profiles suggests
168 that FYN may play a role in general resistance mechanisms against TKI therapy. Consistently, we observed an
169 increase in both protein and mRNA levels of *FYN* following TKI treatment, indicating that upregulation of FYN
170 confers compensatory survival signal in TKI-treated cells (Fig. 3A-B). The phosphorylation levels of FYN was
171 increased proportional to FYN protein level, indicating specific kinase activity of FYN did not change (Fig.
172 S5A). Previous study suggested that increased expression of EGR1 transcription factor is responsible for FYN
173 mRNA accumulation in imatinib resistant CML(18). Consistently, EGR1 expression was increased upon TKI
174 treatment in MDA-MB-231 cells. However, EGR1 expression was not increased in TKI treated MDA-MB-231
175 cells, nor did its knockout significantly downregulated FYN mRNA levels (Fig. S5B). To elucidate the
176 mechanisms underlying the accumulation of *FYN*, we treated MDA-MB-231 cells with inhibitors targeting key
177 epigenetic modifiers and assessed their synergistic effects with NVP-ADW742 in cell killing, as well as their
178 impact on *FYN* mRNA accumulation. Multiple drugs, including pinometostat (DOT1L inhibitor(29)),
179 tazemetostat (EZH2 inhibitor(30)), A366 (G9a inhibitor(31)) and GSK-J4 (KDM6 inhibitor(32)) strongly
180 decreased cell viability upon TKI treatment (Fig. S5C). As the increase in *FYN* mRNA is responsible for TKI
181 resistance, we reasoned that the drug that directly affect FYN mRNA level and hence cell viability should be an
182 inhibitor of epigenetic regulator that enhances transcription. To this end, we focused on pinometostat and GSK-
183 J4 for further validations. Intriguingly, while GSK-J4 decreased FYN mRNA upon NVP-ADW742 treatment,
184 pinometostat failed to decrease it (Fig. S5D).. Consistent with this, treatment with NVP-ADW742 increased the
185 expression of most members of the jumonji domain histone demethylase family (Fig. 3C). This observation is
186 consistent with a previous study on taxane-resistant H1299 lung cancer cells(33), suggesting that histone
187 demethylases may play critical roles in activating a drug resistance gene program. However, the ablation of
188 KDM6, the primary targets of GSK-J4, failed to significantly decrease *FYN* expression (Fig. S5E). GSK-J4 is
189 known to inhibit other jumonji domain histone demethylase family proteins including KDM4 and KDM5(34).
190 Therefore, we tested the possibility that other histone demethylase may be involved in regulating *FYN*
191 expression. Among jumonji domain histone demethylases, *KDM4*, and to a lesser extent *KDM3*, were the only
192 gene family members whose ablation inhibited *FYN* upregulation and p38 activation upon TKI treatment (Figs.
193 3D and S5F). Ablation of KDM5, which has been shown to induce drug tolerance in cancer cells(35), did not

194 significantly alter *FYN* expression (Fig. S5G). Like NVP-ADW742 treatment, gefitinib treatment increased
195 *KDM4* demethylase levels (Fig. S5H). We also analyzed two independent TNBC organoids obtained from
196 primary tumors and found concurrent upregulation of *KDM4* with *FYN* mRNAs upon NVP-ADW742 and
197 gefitinib treatment (Fig. S5I). Critically, time course experiment with NVP-ADW742 treated MDA-MB-231
198 revealed that accumulation of KDM4A protein preceded FYN protein (Fig. 3E), suggesting that KDM4A
199 accumulation may be responsible for FYN accumulation. Both KDM3 and KDM4 demethylates methylated
200 H3K9, thereby promoting the opening heterochromatin for transcription(36). Remarkably, expression of
201 *KDM4A*, the most abundantly expressed gene among KDM4 demethylases in TNBC cell lines (Fig. S6A) was
202 enriched in TNBC compared to other breast cancer subtypes (Fig. 3F) and was positively correlated with *FYN*
203 expression in CCLE database, suggesting that KDM4 regulates *FYN* mRNA levels (Fig. 3G). Genetic ablation
204 of *KDM3* or *KDM4* (Fig. S6B-C) decreased *FYN* and p38 activity. Also, genetic ablation of KDM3 or KDM4
205 sensitizing MDA-MB-231 cells to TKIs (Figs. 3H-I). The Ablation of KDM3 or KDM4 only had modest but
206 statistically insignificant effect on cell viability (Fig. S6D). Likewise, treatment of KDM4 inhibitor QC6352(37)
207 synergized with TKIs in killing MDA-MB-231 cells (Fig. 3J). QC6352 treatment also significantly attenuated
208 *FYN* accumulation upon NVP-ADW742 treatment (Fig. 3K-L). This was consistent with the RNA sequencing
209 data results in the previous study with breast cancer stem cells treated with QC6352(38). Specifically, *FYN* was
210 the most significantly downregulated SRC family kinase upon QC6352 treatment (Fig. 3M). Analysis of
211 chromatin IP (ChIP) sequencing data from the same study revealed KDM4A enrichment near FYN promoter;
212 and QC6352 treatment increased H3K9me3 enrichment at the same locus (Fig. 3N). Indeed, this FYN promoter
213 locus exhibited a reduction in H3K9me3 following NVP-ADW742 treatment, while QC6352 treatment restored
214 H3K9me3 enrichment (Fig. 3O). This finding suggests that KDM4 may directly demethylate H3K9me3 at FYN
215 promoter to upregulate *FYN* transcription. In contrast, H3K27me3 marks, which is demethylated by KDM6
216 family demethylases, were not significantly changed at FYN promoter upon NVP-ADW742 treatment (Fig.
217 S6E). *FYN* accumulation and resistance to TKIs were also confirmed to be attenuated by QC6352 treatment in
218 other independent TNBC cell lines (Figs. S6F-G).

219 **FYN/KDM4 inhibition synergizes with TKI treatment *in vivo***

220 We proceeded to investigate the potential clinical application of our synthetic lethal gene pairs as combinatorial
221 therapy by assessing the *in vivo* efficacy of pharmacological interventions targeting these gene pairs using
222 MDA-MB-231 xenograft models. Strikingly, co-treatment of saracatinib and NVP-ADW742 synergistically

223 reduced tumor size, whereas treatment with either agent alone was ineffective in slowing tumor growth (Fig.
224 4A). All treatment groups exhibited minimal changes in body weight, indicating that the overall health of the
225 animals was not adversely affected by the combination treatment (Fig. S7A). Saracatinib-gefitinib combination
226 was not tested as saracatinib can inhibit EGFR(28). Similarly, KDM4 inhibitor QC6352 synergized with
227 gefitinib in reducing MDA-MB-231 xenograft tumor growth without causing overt changes in animal health
228 (Figs. 4B and S7B). Additionally, the expression levels of *FYN* and *KDM4A* were found to be correlated with
229 poor prognosis in a previously reported breast cancer cohort(24), highlighting the potential of targeting these
230 two genes as therapeutic targets for TNBC (Fig. 4C). Collectively, our results demonstrate that upregulation of
231 *KDM4* upon TKI treatment reduces H3K9me3 mark in *FYN* enhancer, thereby increasing *FYN* expression and
232 promoting cell survival under TKI treatment (Fig. 4D).

233 **FYN is associated with drug tolerant persister phenotype**

234 The observed epigenetic alterations in regulators conferring resistance to multiple cancer drugs closely resemble
235 non-genetic changes associated with the generation of drug-tolerant persisters(35). Indeed, prolonged incubation
236 of MDA-MB-231 cells treated with TKIs or conventional chemotherapy drugs such as doxorubicin or paclitaxel
237 resulted in increased levels of *FYN* (Fig. 5A). Curiously, *KDM4A* expression was only upregulated upon
238 treatment with NVP-ADW742 and gefitinib, suggesting that while *FYN* upregulation is a general feature of drug
239 tolerant cells, the mechanism of *FYN* upregulation may vary depending on the specific drug being used.
240 Analysis of previously published RNA sequencing data from a series of osimertinib tolerant EGFR mutated lung
241 cancer cell lines(39) revealed higher expression levels of *FYN* and *KDM4A* in the drug persisters, but not SRC
242 (Fig. 5B). Consistently, we confirmed upregulation of *FYN* at both the protein and mRNA levels in gefitinib and
243 osimertinib resistant PC9 and HCC827 cells (Figs. 5C-D). Pharmacological inhibition of FYN or
244 downregulation of *FYN* expression through inhibition of KDM4 sensitized gefitinib resistant PC9 cells to EGFR
245 inhibitor, suggesting that *FYN-KDM4* are responsible for gefitinib resistant phenotype in this cell line (Figs.5E-
246 G).

247 Importantly, upregulation of *FYN* has been consistently observed in multiple independent studies involving
248 drug-tolerant cancer cell lines and patient-derived xenografts treated with various drugs that have distinct target
249 profiles, including TKIs (lapatinib, a HER2 inhibitor, against HER2 positive breast cancer(40)) and
250 chemotherapy drugs (irinotecan, topoisomerase inhibitor against colorectal cancer(41); gemcitabine against

251 pancreatic cancer(42); and carboplatin against high grade serous ovarian carcinoma(43)) (Fig. 5H). Moreover,
252 enrichment of *FYN* has also been observed in residual disease following chemotherapy, including neoadjuvant
253 chemostherapy plus bevacizumab treated HER2 negative breast cancer(44), neoadjuvant chemoradiotherapy
254 combined plus atezolizumab treated esophageal cancer(45), and chemoradiotherapy treated colorectal
255 cancer(46), indicating its potential role in mediating drug tolerance during chemotherapy (Fig. 5I). While the
256 causal relationship between FYN expression drug tolerance in response to various therapeutic interventions
257 warrants further study, these evidence suggest that FYN expression is associated with drug tolerance. Notably,
258 an analogous increase in *KDM4* was not consistently observed across all tumor models tested in Figures 5H-I
259 (Fig. S8A-B). This suggests that, as previously noted in Figure 5A, while *FYN* serves as a general mediator of
260 drug tolerance, the specific mechanisms underlying its upregulation may vary depending on the cancer type and
261 the drug being administered. Taken together, these lines of evidence further support our findings in TNBC cell
262 lines and suggest that *FYN* acts as a common mediator of drug tolerance.

263

264 **Discussion**

265 In this study, we employed combinatorial CRISPR screening to identify combinations of TKIs that exhibit
266 synergistic effects in eliminating triple-negative breast cancer (TNBC). We discovered and validated that
267 concurrent targeting of FYN, along with other tyrosine kinases such as IGF1R, EGFR or ABL2 can
268 synergistically eradicate TNBC and impede cancer growth. Our findings also provide evidence that the
269 transcriptional upregulation of *FYN*, facilitated by the activation of KDM4 histone demethylases, confers
270 resistance and persistence to TKIs. Upregulation of *FYN* is a general feature of drug tolerant cancer cells,
271 suggesting the association of *FYN* expression with drug resistance and tumor recurrence after treatment.

272 This research provides basis for breakthrough combinatorial therapy achieving effective targeted therapy with
273 minimal risk of developing resistance. Our combinatorial CRISPR screening demonstrates that treatment with
274 TKIs or histone demethylase inhibitors enhances the sensitivity of cells to other TKIs. Consequently, drug
275 combinations exhibit a more potent inhibition of cancer growth than the simple sum of the therapeutic effects of
276 individual drugs. Furthermore, synergistic drug combinations enable a reduction in the dosage of each drug,
277 with minimal compromise in therapeutic efficacy. Such combinations yield a therapeutic response comparable to
278 that achieved with significantly higher doses of each individual agent. We anticipate that combinatorial therapy

279 has the potential to mitigate side effects by minimizing the dosage of each drug, thus widening the therapeutic
280 window. Further studies should elucidate the downstream mechanisms by which FYN upregulation contributes
281 to drug tolerance. SRC family kinases are known to upregulate multiple signaling pathways including ERK,
282 AKT and p38 pathway(47). Although our study showed that, at least in MDA-MB-231 cell line, FYN depends
283 on p38 activity for TKI resistance (figs. 2J-L), it should further be shown while this downstream mechanism is
284 generalizable in other cancers. The downstream mechanism of p38 that contributes to drug resistance would also
285 be of great interest to identify novel therapeutic approaches minimizing drug tolerance. Also, our combinatorial
286 CRISPR screen results warrant further studies with other synthetic lethal gene combinations other than those
287 involving FYN that are not deeply investigated in this study. Particularly, FGFR2, TEK, FRK identified as key
288 nodes in figure 2C may be of particular interest as they are also associated with cancer cell survival(48, 49).

289 It is intriguing to observe that *FYN* is specifically upregulated in various models of drug resistance and tolerance.
290 SRC family kinases, which includes FYN, have been linked to drug resistance(47, 50). In line with this,
291 phosphoproteomic analysis of neoadjuvant chemotherapy resistant TNBC patient derived xenografts showed
292 upregulated SRC family kinase networks including kinases and their substrates and adaptors(51). Our findings
293 reveal that *FYN* is specifically upregulated at the mRNA level possibly through epigenetic regulations, providing
294 further depth to our understanding of drug resistance in cancer therapy. The epigenetic reprogramming of the
295 drug tolerant cells may be distinct depending on the tumor type or the therapeutic interventions, as KDM4A,
296 which we show is increased upon TKI treatment in TNBC cell line in figure 3, is not significantly regulated in
297 other cancers analyzed in figure 5. Therefore, the context dependent mechanisms underlying FYN upregulation,
298 and its essentiality in constituting drug tolerance remains as subjects for further study.

299 Furthermore, our work highlights the significance of histone demethylases in TKI resistance. Numerous histone
300 demethylases have been implicated in drug resistance and tolerance across different cancer drug types. For
301 instance, the KDM5 family of H3K4 demethylases has been associated with the drug-tolerant persister
302 phenotype against multiple TKIs(35). In our study, we identify *KDM4* as a critical factor in the generation of
303 drug-tolerant persisters in breast cancer. *KDM4* is known to be upregulated in various cancers, including breast
304 cancer, and promotes key malignant traits. Previous studies have demonstrated the essential role of KDM4 in
305 induced pluripotency through its interaction with pluripotency factors(52). These findings suggest that an
306 KDM4 inhibitor could be a promising therapeutic target with specific activity against cancer stem cells.
307 Consistently, specific inhibitors targeting KDM4 have recently been developed and shown to inhibit the

308 generation of breast cancer stem cells(38). The mechanisms underlying KDM4 upregulation upon drug
309 treatment is currently unclear and remains as subjects for further study. Nevertheless, given our discoveries
310 regarding the involvement of *KDM4* in drug resistance in breast and lung cancer, the development of novel
311 drugs targeting KDM4 holds significant therapeutic potential.

312 **Materials and methods**

313 **Cell Culture.** HEK293T, MDA-MB-231, Hs578T cells were obtained from American Type Cell Culture (ATCC)
314 HCC1143, HCC1395, HCC1937 were obtained from Korean cell line bank. HEK293T and MDA-MB-231 were
315 grown in DMEM supplemented with 10% FBS and penicillin/streptomycin. Hs578T and HCC1143, HCC1395,
316 HCC1937 were grown in RPMI1640 supplemented with 10% FBS. Parental and gefitinib-, and Osimertinib-
317 resistant PC9 and HCC827 cells were kind gifts from Jae Cheol Lee (Asan Medical Center, Seoul, Korea) and
318 were grown in RPMI1640 supplemented with 10% FBS. Gefitinib and osimertinib resistant cells are maintained
319 in the presence of 1μM gefitnib and 0.5μM osimertinib, respectively. Gefitinib resistant derivatives of PC9 and
320 HCC827 cells were generated as described previously by treating cells with escalating dose of gefitinib (53). All
321 cell culture medium and supplements are purchased from Welgene Inc.

322 **Combinatorial library construction.** Combinatorial library was constructed as previously described(15). The
323 sgRNAs used in the screens were cloned in pAWp28 storage vector in two versions: one version containing
324 human U6 driven sgRNA with wild type scaffold, and another containing mouse U6 driven sgRNA with cr2
325 variant scaffold. The sgRNA expression cassette consisting of U6 promoter and sgRNA were subject to one-pot,
326 iterative cloning into lentiviral pTK799 vector using BglII-MfeI restriction sites flanking the sgRNA expression
327 cassette and BamHI-EcoRI sites in pTK799. pTK799 vector is derived from pAWp12(15) by replacing CMV-
328 GFP selectable marker to EFS-Puro.

329 **Combinatorial CRISPR screening procedure.** Lentivirus was generated in HEK293T cells by transfecting
330 lentiviral transfer vector, and helper vectors (psPAX2, and pVSV-G) using Fugene HD (Promega). Lentiviral
331 supernatant was collected 48 hours after transfection, and was frozen and stored in -80C. The appropriate titer
332 for lentiviral transduction was determined by transducing MDA-MB231 cells with two-fold serial dilution of
333 lentiviral supernatant, selecting with puromycin 2 days after transduction for 2 days, and determining cell
334 viability with AQuaeous one cell viability, MTS assay (Promega). After determining the titer of lentiviral
335 supernatant, 100 million MDA-MB231 cells carrying constitutively expressed Cas9 were transduced with

336 CombiGEM library at MOI of 0.3. The expected initial coverage is 100 million x 0.3/ (54,289 different sgRNA
337 combinations)= 553. Three days after transduction, the cells were either harvested as day 0 sample or selected
338 with 2μg/mL puromycin (Invitrogen). Cells were treated with benzonase before harvesting to minimize
339 carryover of plasmid DNA in lentiviral supernatant. Cells were grown in the presence of 2μg/mL puromycin for
340 20 days before harvesting.

341 The genomic DNA of harvested cells were isolated using Blood & Cell Culture Maxi kit (Qiagen). The PCR
342 amplicon spanning the two sgRNAs were generated with PCR using Q5 High Fidelity DNA polymerase (New
343 England Biolabs) and the following primers:

344 F: CAAGCAGAAGACGGCATACGAGAT CCTAGTAACTATAGAGGCTTAATGTGCG

345 R: AATGATACGGCGACCACCGAGATCTACAC NNNNNN ACACGAATTCTGCCGTGGATCCAA

346 The six nucleotides described as "NNNNNN" in reverse primer above represents unique index to identify
347 biological replicates in multiplexed NGS run.

348 The PCR protocol involves 60 seconds of initial DNA denaturation at 98C, and 20 cycles of 10 seconds
349 denaturation at 98C, 10 seconds annealing at 67C, and 120 seconds elongation at 72C. All genomic DNA
350 isolated were used in PCR reaction at concentration of 40μg/mL. All PCR products were combined and
351 precipitated with isopropanol at room temperature. The precipitated DNA was resuspended in 400μL EB buffer
352 (Qiagen) and gel purified. The purified PCR products were sent for NGS by NextSeq500 paired end sequencing
353 with the following sequencing primers:

354 Forward read: GGACTAGCCTTATTTGAACTTGCTATGCAGCTTTCTGCTTAGCTCTCAAAC

355 Forward index read:
356 CGGTGCCACTTTTTCAAGTTGATAACGGACTAGCCTTATTTTAACTTGCTATTTCTAGCTCTAAAAC

357 Reverse read: GCA CCG AGT CGG TGC TTT TTT GGA TCC ACG GCA GAA TTC GTGT

358 The raw GI scores calculated as deviation from the quadratic fit of the expected-observed Z score plot. The GI
359 scores were normalized by dividing the raw GI scores with the standard deviation of the GI scores obtained
360 from the 200 nearest neighbors in terms of expected Z scores (Fig. S1I)(11).

361 **Data analysis.** The sgRNA sequences were identified and their occurrences were counted with C++ script
362 deposited in Github (https://github.com/tackhoonkim/combinatorial-CRISPR-screens-2023).

363 **Validation of screens using sgRNAs.** Individual sgRNA was cloned to either pTK1329, and pTK1336 that are
364 both derived from pAWp12 with EFS-GFP and EFS-mCherry, respectively, as selectable markers. Validation of
365 synthetic lethality between gene A and B were analyzed by transducing MDA-MB-231 Cas9 cells with four
366 combinations of lentiviral supernatant pairs (MOI ~ 0.5 each) containing (1) GFP-sgA and mCherry-sgB; (2)
367 GFP-sgA and mCherry-sgCon; (3) GFP-sgCon and mCherry-sgB; (4) GFP-sgCon and mCherry-sgCon. The
368 fraction of GFP/mCherry double positive cells were analyzed using BD Accuri C6 and its accompanying
369 software. The expected fold change in sgA+sgB were calculated as $FC_{sgA+sgCon}$ x $FC_{sgCon+sgB}$, where FC is
370 normalized fold change in fraction of GFP/mCherry double positive cells relative to those transduced with GFP-
371 sgCon and mCherry-sgCon.

372 **MTT Cell viability assay.** Cells were seeded at 1000-2000 cells/well in 96 well plate. Tyrosine kinase inhibitors
373 at indicated combination of dose were treated 12 hours after seeding, and cells were grown for 3 days. The
374 relative viability was measured by EzCytox cell viability assay (Dojindo). The absorbance at 450nm wavelength
375 was measured using EnVision multimode plate reader (PerkinElmer).

376 **Cell death and cell proliferation assay.** Cells were incubated with tyrosine kinase inhibitors for 48 hours. Cell
377 proliferation was quantified with BrdU assay using FITC conjugated BrdU antibody (Biolegend, 364103) and
378 propidum iodide/RNase A solution (Cell Signaling), analyzed with BD Accuri C6 and accompanied software.
379 Cell death was quantified with Live-Dead cell staining kit (Molecular Probes) by flow cytometry analysis using
380 BD Accuri C6 and accompanied software.

381 **Western blot analysis.** Cells were treated with drugs for 48 hours unless otherwise indicated. Western blots
382 were performed as previously reported. Briefly, Cells were lysed in RIPA buffer (50mM Tris-HCl pH 7.5,
383 150mM sodium chloride, 0.1% sodium dodecyl sulfate, 0.5% sodium deoxycholate, 1% NP-40, 1mM EDTA)
384 supplemented with protease inhibitor (aprotinin, leupeptin, pepstatin A, and phenylmethylsulfonyl fluoride
385 [PMSF]) and phosphatase inhibitor (sodium fluoride and sodium orthovanadate) cocktail. Antibodies used for
386 western blot analysis were: anti-SRC (Santa Cruz biotechnology, mouse sc-), anti-FYN (Cell Signaling
387 Technology, rabbit #4023), anti-phospho-FYN Y530 (Invitrogen, PA5-36644), anti-GAPDH (Cell Signaling
388 Technology, rabbit #5174), anti-KDM4A (Bethyl Laboratories, rabbit A300-861A), anti-phospho-ERK

389 T202/Y204 (Cell Signaling Technology, rabbit #9101), anti-ERK (Cell Signaling Technology, rabbit #9102),
390 anti-phospho-STAT3 Y705 (Cell Signaling Technology, rabbit #9145), anti-STAT3 (Cell Signaling Technology,),
391 anti-phospho-AKT (Cell Signaling Technology, mouse #4051), anti-AKT (Cell Signaling Technology,), anti-
392 phospho-p38 (Cell Signaling Technology,), anti-p38 (Cell Signaling Technology,).

393 **RT-qPCR analysis**. RNA is extracted from cultured cells with Trizol (Invitrogen) according to the
394 manufacturer's instructions. The precipitated RNA pellet was resuspended in RNase free water (Enzynomics),
395 and was subject to reverse transcription with M-MLV reverse transcriptase (Enzynomics) at 37C for 2 hours,
396 followed by heat inactivation at 95C for 5 minutes. The resulting cDNA was used for quantitative real time PCR
397 using TOPreal SYBR Green qPCR premix (low ROX, Enzynomics) reagent and CFX96 Real-Time PCR
398 detection system (Bio-Rad).

399 **Xenograft assay.** All animal experiments were approved by IACUC of Korea Institute of Science and
400 Technology (KIST). Six-week-old female nude mice were injected with 5 x 10^6 MDA-MB-231 cells suspended
401 in 1:1 (w/w) mixture of PBS and growth factor reduced Matrigel (Corning) in fourth inguinal mammary fat pad.
402 Starting two weeks after tumor cell injection, saracatinib (50mg/kg mouse body weight, MedChemExpress),
403 NVP-ADW742 (20mg/kg, Sigma), gefitinib (20mg/kg, MedChemExpress), QC6352 (10mg/kg,
404 MedChemExpress) in 45% saline+40% polyethyleneglycol 300 (sigma)+5% Tween-80 (sigma)+5% DMSO
405 (sigma) were injected intraperitoneally every 24 hours for two weeks. Tumor volume was measured by digital
406 caliper and calculated as $(\text{width})^2$ x length x 0.5.

407 **Public database analyses.** Gene Expression Omnibus (GEO) data with breast cancer cohort (GSE25066(24))
408 were analyzed using web based platform Cancer Target Gene Screening (https://ctgs.biohackers.net)(54). Cancer
409 Cell Line Encyclopedia (CCLE) data were analyzed using depmap R package version 1.14. The list of GEO data
410 used for analysis are listed in table S2.

411 **Primary TNBC organoid culture and drug treatment.** Specimens was obtained from enrolled patients with
412 TNBC breast cancer with IRB approval. Tumor tissue was collected and transferred using cold RPMI1640
413 media at the National Cancer Center (Goyang, Republic of Korea). Then the tissues were dissected with a blade
414 on Petri dish and enzymatically digested with dissociated kit (Multi Tissue Dissociation Kit 1, 130-110-201) by
415 gentle MACS Dissociators (Miltenyi Biotec, Germany). After cell counting, 1 × 10^5 cells were embedded in 40

416 μl of Matrigel (Corning) and seeded into each well of a 24-well cell culture plate. After the matrigel was
417 solidified, 500 μL organoid medium supplemented with advanced DMEM/F12 medium (Invitrogen, USA), B27
418 (Invitrogen, USA, 17504), 1.25 mM N-acetylcysteine (Sigma, USA, A9165), 5 ng/mL EGF (PeproTech, USA,
419 AF-100-15), 20 ng/mL FGF-10 (Peprotech, 100-26), 5ng/ml FGF7 (Peprotech, AF-100-19), 50ng/ml R-spondin
420 1 (Qkine, Qk006), 5 mM nicotinamide (Sigma, N0636), 500 nM A83-01 (Tocris, 2939), 1X GlutaMAX (Gibco,
421 35050-061), 100ug/ml primocin (Invivogen, ant-pm), 10mM HEPES (Gibco, 15630-080), 1X Noggin (U-
422 Protein Express BV, N002), 1X ITS (Gibco, 12585014), 100nM β-estradiol (Sigma, E2758), 1ug/ml
423 Hydrocortisone (Sigma, H0888), 5nM Heregulin (PeproTech, AF-100-03), 500nM SB202190 (R&D system,
424 1264), 10uM Y27632 (TOCRIS, 1254) as described by Clevers and colleagues (55), was added to each well and
425 the cells grown under standard culture conditions (37 ℃, 5% CO2).

426 **Acknowledgments.**

427 We thank BioMicro Center of MIT for sequencing analysis. We thank Jae Cheol Lee (Asan Medical Center,
428 Korea) for providing gefitinib resistant lung cancer cell lines. This work was supported by Korea Institute of
429 Science and Technology (KIST) Institutional Programs (2E32331 to T.K.); and National Research Foundation of
430 Korea, funded by the Korean government (MSIT) (2021R1A2C1093499 to T.K., 2020M3A9A5036362 to
431 S.Y.K).

432 **Author contributions.** T.K., B.-S.P., H.J. and J.K. performed experiments. T.K. and T.K.L. supervised the
433 research. S.H. S.-Y.J. and S.Y.K. performed experiments with TNBC patient derived organoids. D.K., S.K.L.
434 generated and provided osimertinib resistant HCC827 cell line.

435 **Conflict of Interest Statement**

436 The authors declare no conflict of interest

437 **Ethics Statement**

438 All experiments with human tumor organoids were conducted in accordance with the requirements of the
439 National Cancer Center Institutional Review Board (IRB).

Availability of data and materials: The NGS data for CRISPR screening results are available under NCBI SRA accession code PRJNA976939.

References

1. Wu P, Nielsen TE, Clausen MH. Small-molecule kinase inhibitors: an analysis of FDA-approved drugs. Drug Discovery Today. 2016;21(1):5-10.
2. Hanahan D, Weinberg Robert A. Hallmarks of Cancer: The Next Generation. Cell. 2011;144(5):646-74.
3. Li Y, Zhan Z, Yin X, Fu S, Deng X. Targeted Therapeutic Strategies for Triple-Negative Breast Cancer. Frontiers in Oncology. 2021;11.
4. Litzenburger BC, Creighton CJ, Tsimelzon A, Chan BT, Hilsenbeck SG, Wang T, et al. High IGF-IR Activity in Triple-Negative Breast Cancer Cell Lines and Tumorgrafts Correlates with Sensitivity to Anti–IGF-IR Therapy. Clinical Cancer Research. 2011;17(8):2314-27.
5. Morgillo F, Della Corte CM, Fasano M, Ciardiello F. Mechanisms of resistance to EGFR-targeted drugs: lung cancer. ESMO Open. 2016;1(3):e000060.
6. Maemondo M, Inoue A, Kobayashi K, Sugawara S, Oizumi S, Isobe H, et al. Gefitinib or Chemotherapy for Non–Small-Cell Lung Cancer with Mutated EGFR. New England Journal of Medicine. 2010;362(25):2380-8.
7. Leonetti A, Sharma S, Minari R, Perego P, Giovannetti E, Tiseo M. Resistance mechanisms to osimertinib in EGFR-mutated non-small cell lung cancer. British Journal of Cancer. 2019;121(9):725-37.
8. Jin H, Wang L, Bernards R. Rational combinations of targeted cancer therapies: background, advances and challenges. Nature Reviews Drug Discovery. 2023;22(3):213-34.
9. Wong ASL, Choi GCG, Cui CH, Pregernig G, Milani P, Adam M, et al. Multiplexed barcoded CRISPR-Cas9 screening enabled by CombiGEM. Proceedings of the National Academy of Sciences. 2016;113(9):2544-9.
10. Horlbeck MA, Xu A, Wang M, Bennett NK, Park CY, Bogdanoff D, et al. Mapping the Genetic Landscape of Human Cells. Cell. 2018;174(4):953-67.e22.
11. Han K, Jeng EE, Hess GT, Morgens DW, Li A, Bassik MC. Synergistic drug combinations for cancer identified in a CRISPR screen for pairwise genetic interactions. Nature Biotechnology. 2017;35(5):463-74.
12. Shen JP, Zhao D, Sasik R, Luebeck J, Birmingham A, Bojorquez-Gomez A, et al. Combinatorial CRISPR–Cas9 screens for de novo mapping of genetic interactions. Nature Methods. 2017;14(6):573-6.
13. Corsello SM, Bittker JA, Liu Z, Gould J, McCarren P, Hirschman JE, et al. The Drug Repurposing Hub: a next-generation drug library and information resource. Nature medicine.

476 2017;23(4):405-8.
477 14. Doench JG, Fusi N, Sullender M, Hegde M, Vaimberg EW, Donovan KF, et al. Optimized
478 sgRNA design to maximize activity and minimize off-target effects of CRISPR-Cas9. Nature
479 Biotechnology. 2016;34(2):184-91.
480 15. Wong ASL, Choi GCG, Cheng AA, Purcell O, Lu TK. Massively parallel high-order
481 combinatorial genetics in human cells. Nat Biotech. 2015;33(9):952-61.
482 16. Luo B, Cheung HW, Subramanian A, Sharifnia T, Okamoto M, Yang X, et al. Highly parallel
483 identification of essential genes in cancer cells. Proceedings of the National Academy of Sciences.
484 2008;105(51):20380.
485 17. Stein PL, Vogel H, Soriano P. Combined deficiencies of Src, Fyn, and Yes tyrosine kinases
486 in mutant mice. Genes & Development. 1994;8(17):1999-2007.
487 18. Irwin ME, Johnson BP, Manshouri R, Amin HM, Chandra J. A NOX2/Egr-1/Fyn pathway
488 delineates new targets for TKI-resistant malignancies. Oncotarget. 2015;6(27).
489 19. Fenouille N, Puissant A, Dufies M, Robert G, Jacquel A, Ohanna M, et al. Persistent
490 Activation of the Fyn/ERK Kinase Signaling Axis Mediates Imatinib Resistance in Chronic
491 Myelogenous Leukemia Cells through Upregulation of Intracellular SPARC. Cancer Research.
492 2010;70(23):9659-70.
493 20. Airiau K, Turcq B, Mahon F-X, Belloc F. A new mechanism of resistance to ABL1 tyrosine
494 kinase inhibitors in a BCR-ABL1-positive cell line. Leukemia Research. 2017;61:44-52.
495 21. Grosso S, Puissant A, Dufies M, Colosetti P, Jacquel A, Lebrigand K, et al. Gene expression
496 profiling of imatinib and PD166326-resistant CML cell lines identifies Fyn as a gene associated
497 with resistance to BCR-ABL inhibitors. Molecular Cancer Therapeutics. 2009;8(7):1924-33.
498 22. Lee G-H, Yoo K-C, An Y, Lee H-J, Lee M, Uddin N, et al. FYN promotes mesenchymal
499 phenotypes of basal type breast cancer cells through STAT5/NOTCH2 signaling node. Oncogene.
500 2018;37(14):1857-68.
501 23. Xie Y-G, Yu Y, Hou L-K, Wang X, Zhang B, Cao X-C. FYN promotes breast cancer
502 progression through epithelial-mesenchymal transition. Oncol Rep. 2016;36(2):1000-6.
503 24. Hatzis C, Pusztai L, Valero V, Booser DJ, Esserman L, Lluch A, et al. A Genomic Predictor of
504 Response and Survival Following Taxane-Anthracycline Chemotherapy for Invasive Breast Cancer.
505 JAMA. 2011;305(18):1873-81.
506 25. Ghandi M, Huang FW, Jané-Valbuena J, Kryukov GV, Lo CC, McDonald ER, et al. Next-
507 generation characterization of the Cancer Cell Line Encyclopedia. Nature. 2019;569(7757):503-8.
508 26. Hanke JH, Gardner JP, Dow RL, Changelian PS, Brissette WH, Weringer EJ, et al. Discovery
509 of a Novel, Potent, and Src Family-selective Tyrosine Kinase Inhibitor: STUDY OF Lck- AND FynT-
510 DEPENDENT T CELL ACTIVATION. 1996;271(2):695-701.
511 27. Zheng S, Wang W, Aldahdooh J, Malyutina A, Shadbahr T, Tanoli Z, et al. SynergyFinder
512 Plus: Toward Better Interpretation and Annotation of Drug Combination Screening Datasets.
513 Genomics, Proteomics & Bioinformatics. 2022;20(3):587-96.
514 28. Green TP, Fennell M, Whittaker R, Curwen J, Jacobs V, Allen J, et al. Preclinical anticancer

515 activity of the potent, oral Src inhibitor AZD0530. Molecular Oncology. 2009;3(3):248-61.
516 29. Daigle SR, Olhava EJ, Therkelsen CA, Basavapathruni A, Jin L, Boriack-Sjodin PA, et al.
517 Potent inhibition of DOT1L as treatment of MLL-fusion leukemia. Blood. 2013;122(6):1017-25.
518 30. Knutson SK, Warholic NM, Wigle TJ, Klaus CR, Allain CJ, Raimondi A, et al. Durable tumor
519 regression in genetically altered malignant rhabdoid tumors by inhibition of methyltransferase
520 EZH2. Proceedings of the National Academy of Sciences. 2013;110(19):7922-7.
521 31. Sweis RF, Pliushchev M, Brown PJ, Guo J, Li F, Maag D, et al. Discovery and Development
522 of Potent and Selective Inhibitors of Histone Methyltransferase G9a. ACS Medicinal Chemistry
523 Letters. 2014;5(2):205-9.
524 32. Kruidenier L, Chung C-w, Cheng Z, Liddle J, Che K, Joberty G, et al. A selective jumonji
525 H3K27 demethylase inhibitor modulates the proinflammatory macrophage response. Nature.
526 2012;488(7411):404-8.
527 33. Dalvi MP, Wang L, Zhong R, Kollipara RK, Park H, Bayo J, et al. Taxane-Platin-Resistant
528 Lung Cancers Co-develop Hypersensitivity to JumonjiC Demethylase Inhibitors. Cell Reports.
529 2017;19(8):1669-84.
530 34. Heinemann B, Nielsen JM, Hudlebusch HR, Lees MJ, Larsen DV, Boesen T, et al. Inhibition
531 of demethylases by GSK-J1/J4. Nature. 2014;514(7520):E1-E2.
532 35. Sharma SV, Lee DY, Li B, Quinlan MP, Takahashi F, Maheswaran S, et al. A Chromatin-
533 Mediated Reversible Drug-Tolerant State in Cancer Cell Subpopulations. Cell. 2010;141(1):69-80.
534 36. Hyun K, Jeon J, Park K, Kim J. Writing, erasing and reading histone lysine methylations.
535 Experimental & Molecular Medicine. 2017;49(4):e324-e.
536 37. Chen YK, Bonaldi T, Cuomo A, Del Rosario JR, Hosfield DJ, Kanouni T, et al. Design of
537 KDM4 Inhibitors with Antiproliferative Effects in Cancer Models. ACS Medicinal Chemistry Letters.
538 2017;8(8):869-74.
539 38. Metzger E, Stepputtis SS, Strietz J, Preca B-T, Urban S, Willmann D, et al. KDM4 Inhibition
540 Targets Breast Cancer Stem–like Cells. Cancer Research. 2017;77(21):5900-12.
541 39. Gogleva A, Polychronopoulos D, Pfeifer M, Poroshin V, Ughetto M, Martin MJ, et al.
542 Knowledge graph-based recommendation framework identifies drivers of resistance in EGFR
543 mutant non-small cell lung cancer. Nature Communications. 2022;13(1):1667.
544 40. Chang CA, Jen J, Jiang S, Sayad A, Mer AS, Brown KR, et al. Ontogeny and Vulnerabilities
545 of Drug-Tolerant Persisters in HER2+ Breast Cancer. Cancer Discovery. 2022;12(4):1022-45.
546 41. Rehman SK, Haynes J, Collignon E, Brown KR, Wang Y, Nixon AML, et al. Colorectal
547 Cancer Cells Enter a Diapause-like DTP State to Survive Chemotherapy. Cell. 2021;184(1):226-
548 42.e21.
549 42. Liu Y, Azizian NG, Sullivan DK, Li Y. mTOR inhibition attenuates chemosensitivity through
550 the induction of chemotherapy resistant persisters. Nature Communications. 2022;13(1):7047.
551 43. du Manoir S, Delpech H, Orsetti B, Jacot W, Pirot N, Noel J, et al. In high-grade ovarian
552 carcinoma, platinum-sensitive tumor recurrence and acquired-resistance derive from quiescent
553 residual cancer cells that overexpress CRYAB, CEACAM6, and SOX2. The Journal of Pathology.

2022;257(3):367-78.
44. Kimbung S, Markholm I, Bjöhle J, Lekberg T, von Wachenfeldt A, Azavedo E, et al. Assessment of early response biomarkers in relation to long-term survival in patients with HER2-negative breast cancer receiving neoadjuvant chemotherapy plus bevacizumab: Results from the Phase II PROMIX trial. International Journal of Cancer. 2018;142(3):618-28.
45. van den Ende T, de Clercq NC, van Berge Henegouwen MI, Gisbertz SS, Geijsen ED, Verhoeven RHA, et al. Neoadjuvant Chemoradiotherapy Combined with Atezolizumab for Resectable Esophageal Adenocarcinoma: A Single-arm Phase II Feasibility Trial (PERFECT). Clinical Cancer Research. 2021;27(12):3351-9.
46. Snipstad K, Fenton CG, Kjæve J, Cui G, Anderssen E, Paulssen RH. New specific molecular targets for radio-chemotherapy of rectal cancer. Molecular Oncology. 2010;4(1):52-64.
47. Zhang S, Yu D. Targeting Src family kinases in anti-cancer therapies: turning promise into triumph. Trends in Pharmacological Sciences. 2012;33(3):122-8.
48. Formisano L, Lu Y, Servetto A, Hanker AB, Jansen VM, Bauer JA, et al. Aberrant FGFR signaling mediates resistance to CDK4/6 inhibitors in ER+ breast cancer. Nature Communications. 2019;10(1):1373.
49. Zhang L, Yang Y, Chai L, Bu H, Yang Y, Huang H, et al. FRK plays an oncogenic role in non-small cell lung cancer by enhancing the stemness phenotype via induction of metabolic reprogramming. International Journal of Cancer. 2020;146(1):208-22.
50. Girotti MR, Pedersen M, Sanchez-Laorden B, Viros A, Turajlic S, Niculescu-Duvaz D, et al. Inhibiting EGF Receptor or SRC Family Kinase Signaling Overcomes BRAF Inhibitor Resistance in Melanoma. Cancer Discovery. 2013;3(2):158-67.
51. Kohale IN, Yu J, Zhuang Y, Fan X, Reddy RJ, Sinnwell J, et al. Identification of Src Family Kinases as Potential Therapeutic Targets for Chemotherapy-Resistant Triple Negative Breast Cancer. Cancers [Internet]. 2022; 14(17).
52. Loh Y-H, Zhang W, Chen X, George J, Ng H-H. Jmjd1a and Jmjd2c histone H3 Lys 9 demethylases regulate self-renewal in embryonic stem cells. Genes & Development. 2007;21(20):2545-57.
53. Zhang Z, Lee JC, Lin L, Olivas V, Au V, LaFramboise T, et al. Activation of the AXL kinase causes resistance to EGFR-targeted therapy in lung cancer. Nature Genetics. 2012;44(8):852-60.
54. Kim H-Y, Choi H-J, Lee J-Y, Kong G. Cancer Target Gene Screening: a web application for breast cancer target gene screening using multi-omics data analysis. Briefings in Bioinformatics. 2020;21(2):663-75.
55. Sachs N, de Ligt J, Kopper O, Gogola E, Bounova G, Weeber F, et al. A Living Biobank of Breast Cancer Organoids Captures Disease Heterogeneity. Cell. 2018;172(1):373-86.e10.

591

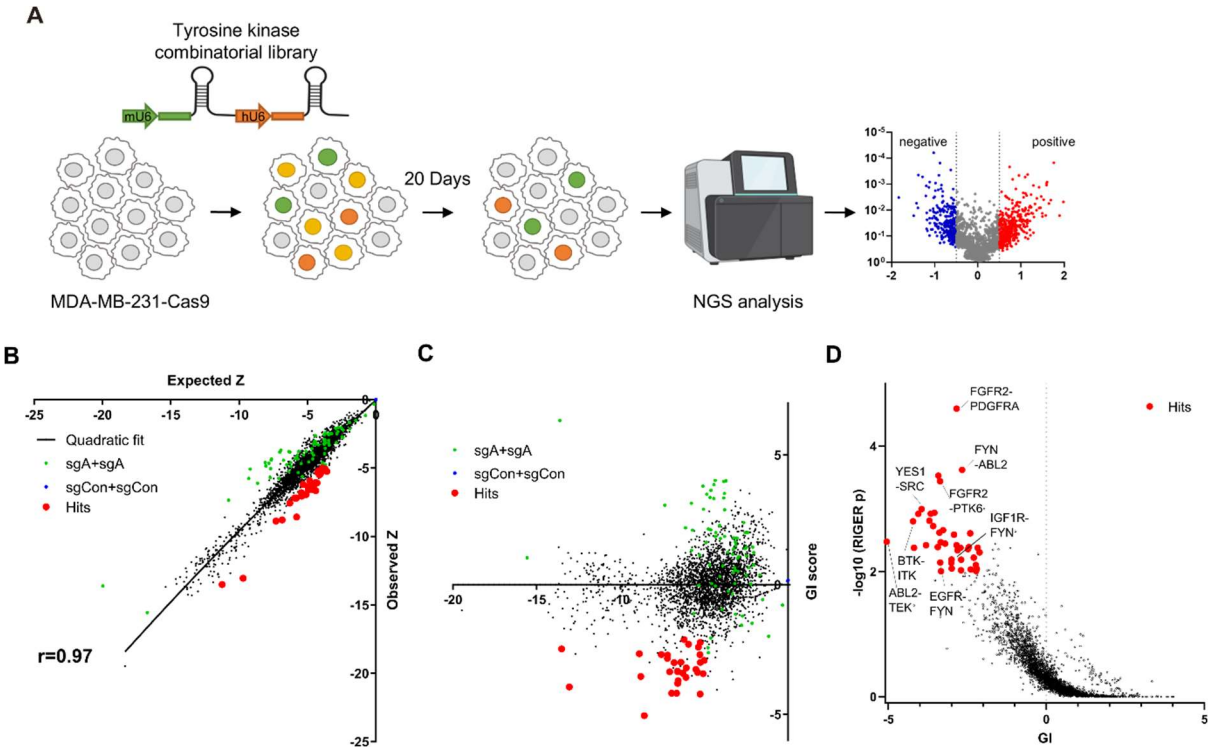

592 **Figure 1. Pairwise CRISPR screen reveals combinations of synthetic lethal tyrosine kinase ablations.** (A)
593 Schematic diagram of combinatorial screens performed in TNBC cell line MDA-MB-231. (B) Scatter plot of
594 expected growth phenotype Z score and observed growth phenotype Z score of each gene combination. Green
595 dots indicate gene combinations where the identical gene is targeted by the two sgRNAs. Red dots indicate
596 candidate synthetic lethal gene pairs listed in table S1. (C) Scatter plot of growth phenotype Z score and
597 normalized GI score of each gene combination. (D) Scatter plot of gene level GI score and RIGER p value
598 calculated with GI scores of each sgRNA pairs that target the given gene pair.

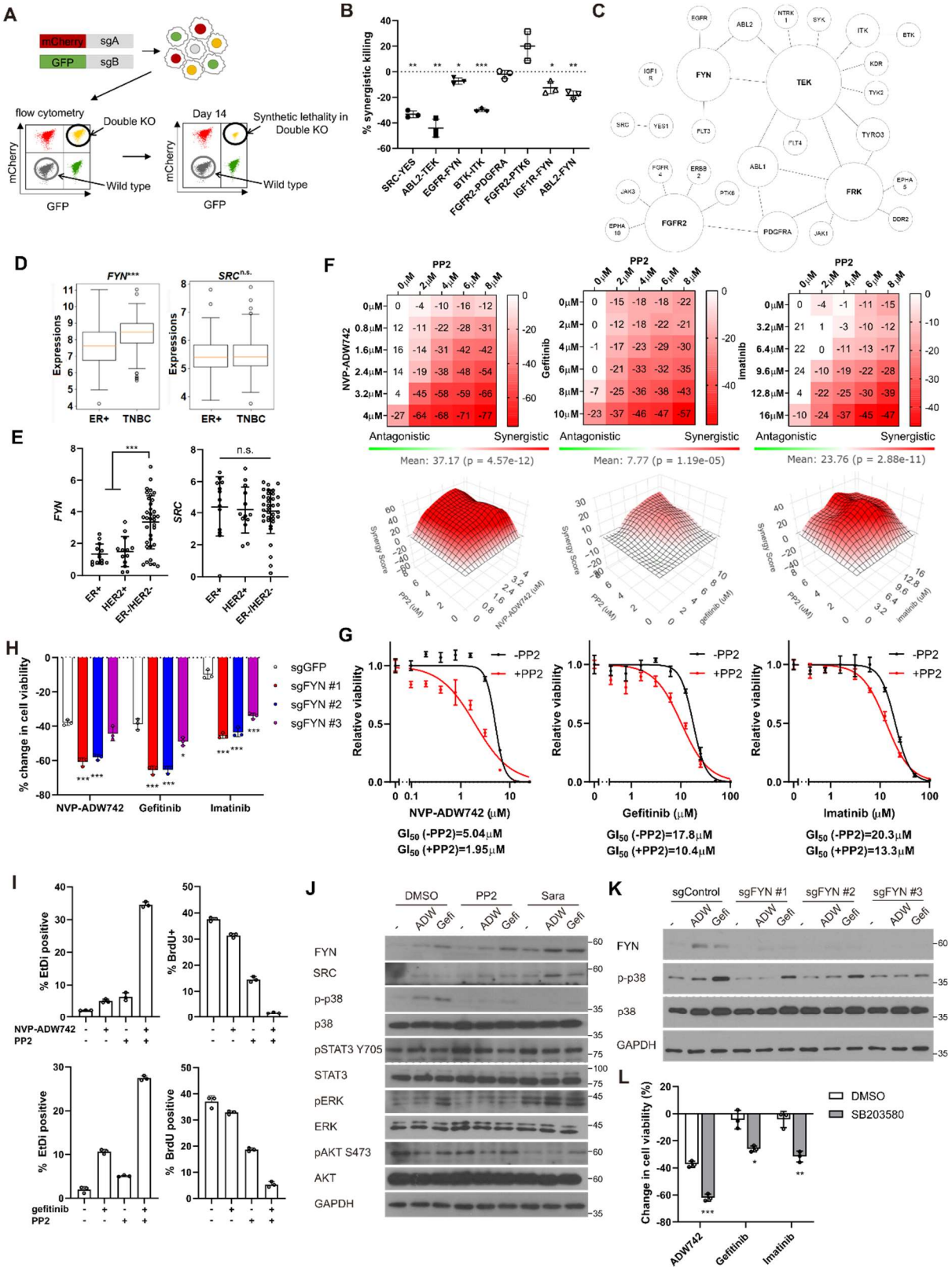

Figure 2. FYN is critical mediator of TKI resistance. (A) Schematic diagram of *in vitro* validation of synthetic lethal gene pairs using sgRNAs. (B) Summary of synergistic killing by sgRNAs targeting indicated gene pairs (n=3). (C) Network analysis of the 30 candidate synthetic lethal gene pairs highlighted in figure 1D.

603 The size of each node is manually drawn to be proportional to the number of connections the gene has. (D-E)
604 *FYN* and SRC mRNA expressions in (D) microarray data of primary breast cancers of GSE25066 cohort, and (E)
605 in cancer cell line encyclopedia, for indicated subtypes. (F) Summary of MTT assay with MDA-MB-231 cells
606 treated with the TKI combinations at indicated concentrations (n=2). Synergistic killing is calculated using
607 SynergyFinder with Bliss independence model. (G) Dose response curve of the indicated TKI in the presence
608 and absence of 5μM PP2 treated for 72 hours (n=3). (H) MTT assay with MDA-MB-231 Cas9 cells expressing
609 indicated sgRNAs treated with indicated TKIs for 72 hours (n=3). (I) Cell death and cell proliferation in MDA-
610 MB-231 cells treated with NVP-ADW742, gefitinib and PP2 either as single agent or as combination for 72
611 hours (n=3). (J) western blot analysis of MDA-MB-231 cells treated with indicated drugs for 48 hours (K)
612 western blot analysis of MDA-MB-231 Cas9 cells expressing indicated sgRNA and treated with indicated drugs
613 for 48 hours. (L) MTT assay of MDA-MB-231 cells treated with indicated drugs for 72 hours (SB203580: 10μ
614 M, NVP-ADW742: 4μM, gefitinib: 10μM, imatinib: 10μM) (n=3). PP2, Saracatinib, NVP-ADW742, gefitinib
615 and imatinib were treated at 5μM, 5μM, 4μM, 12μM, 12μM unless otherwise indicated. All data are plotted as
616 mean±s.d. One sample t-test for B, and unpaired two-sided Student's t-test in D,E,H and L. *, $p<0.05$; **,
617 $p<0.01$; ***, $p<0.001$; n.s., $p>0.05$. All replicates are biological replicates.

618

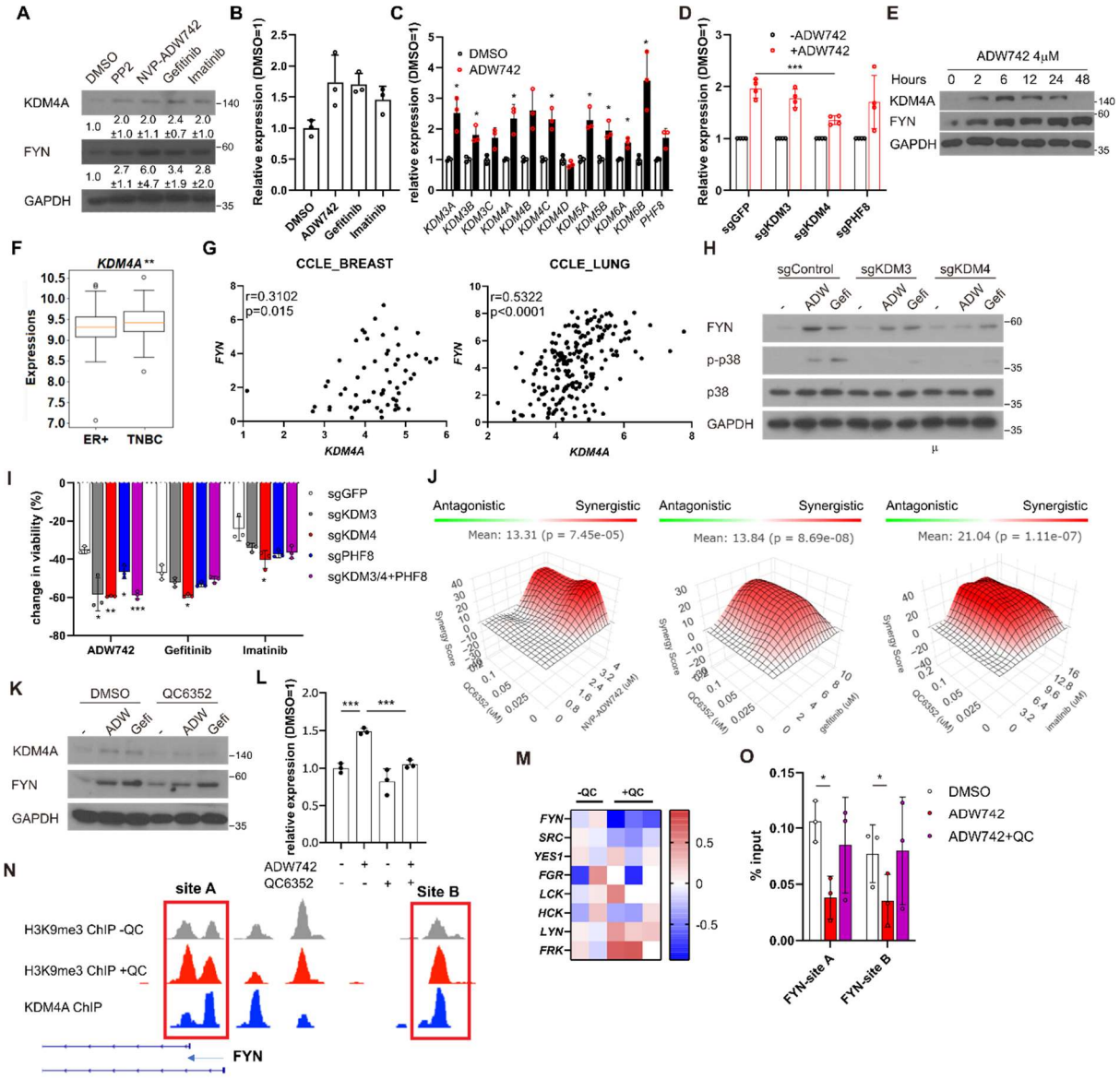

619

620 **Figure 3. Activation of *KDM4* upregulates *FYN*, conferring drug resistance.** (A) Western blot analysis of
621 MDA-MB-231 cells treated with indicated drugs. Numbers below blots indicate quantification of average±s.d.
622 expression level normalized to GAPDH in three independent experiments. (B) RT-qPCR analysis of *FYN*
623 expression levels in MDA-MB-231 cells treated with indicated drugs for 48 hours (n=3). (C) RT-qPCR analysis
624 of indicated jumonji family histone demethylase expression levels after 48 hours treatment of NVP-ADW742
625 (n=3). (D) Changes in *FYN* mRNA levels upon 48 hours of NVP-ADW742 treatment in MDA-MB-231 Cas9
626 cells expressing indicated sgRNAs (n=4). (E) *KDM4A* mRNA levels in primary tumor tissues of indicated
627 subtypes in GSE25066 cohort. (F) Positive correlation of *FYN* and *KDM4A* mRNA levels in CCLE database. (G)
628 western blot analysis of MDA-MB-231 Cas9 cells expressing indicated sgRNA and treated with indicated drugs
629 for 48 hours. (H) MTT assay of MDA-MB-231 Cas9 cells expressing indicated sgRNAs and treated with

630 indicated drugs for 72 hours (n=3). (I) SynergyFinder analysis of MDA-MB-231 cells treated with indicated
631 drug combinations (n=2). (J-K) western blot analysis (J) and RT-qPCR analysis (K) of MDA-MB-231 cells
632 treated with indicated drugs for 48 hours (n=3). (L) mRNA expression levels of SRC family kinases in breast
633 cancer stem cells treated with QC6352 in RNA sequencing data described in Metzger et. al.(38) (M) H3K9me3
634 and KDM4A enrichment at genomic locus encoding *FYN* promoter in ChIP sequencing data described in the
635 same study as (L). (N) H3K9me3 Chromatin immunoprecipitation-qPCR analysis of MDA-MB-231 cells
636 treated with indicated drug for 48 hours at specified genomic loci (n=3). QC6352, PP2, NVP-ADW742,
637 gefitinib and imatinib were treated at 10μM, 5μM, 4μM, 12μM, 12μM , respectively, unless otherwise indicated.

638 All data are plotted as mean±s.d. Unpaired two-sided Student's t-test in B,C,D,E,H and K. Paired two-sided
639 Student's t-test in N. *, $p<0.05$; **, $p<0.01$; ***, $p<0.001$; n.s., $p>0.05$. All replicates are biological replicates.

640

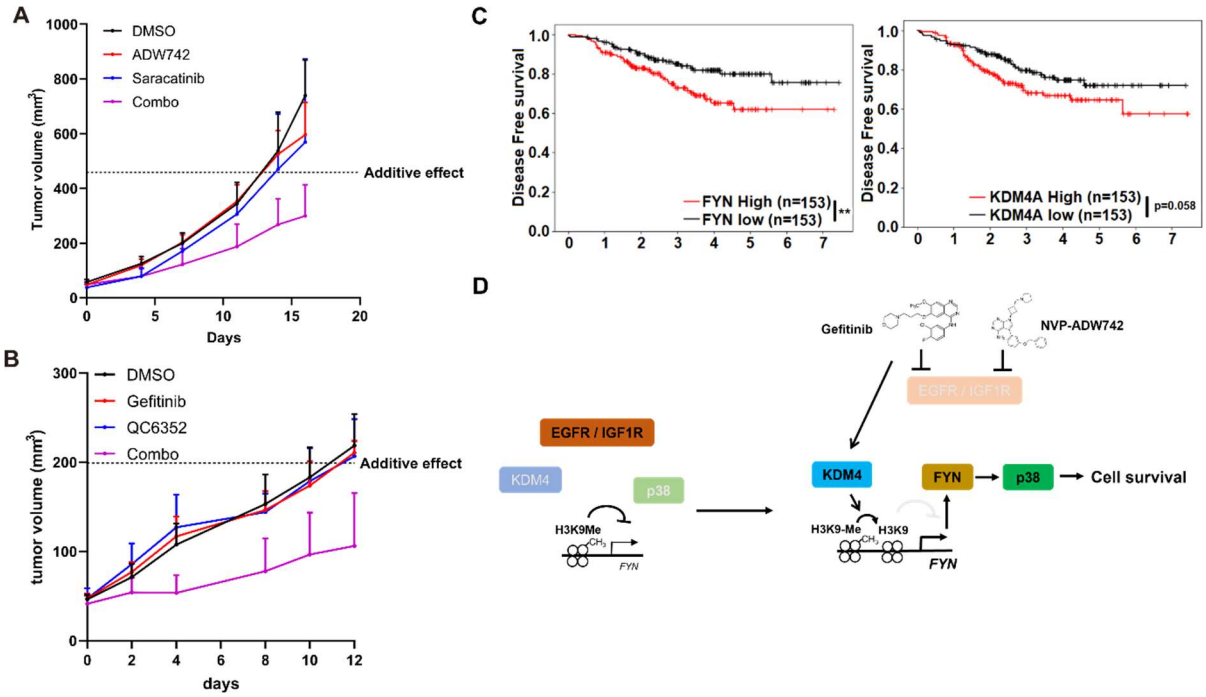

641

642 **Figure 4. Combination therapy targeting FYN+IGF1R and KDM4+EGFR synergistically eliminates**
643 **tumor *in vivo*.** (A-B) Tumor volume for MDA-MB-231 xenografts treated with indicated drugs. Additive effects
644 were calculated by Bliss independence model (n=5). (C) Distant relapse free survival of GSE25066 patient
645 cohort classified by *FYN* (left) and *KDM4A* (right) mRNA expression. (D) Schematics diagram of the
646 mechanism of KDM4-FYN conferring TKI resistance. All data are plotted as mean±s.d. *, $p<0.05$; **, $p<0.01$;
647 ***, $p<0.001$; n.s., $p>0.05$. All replicates are biological replicates.

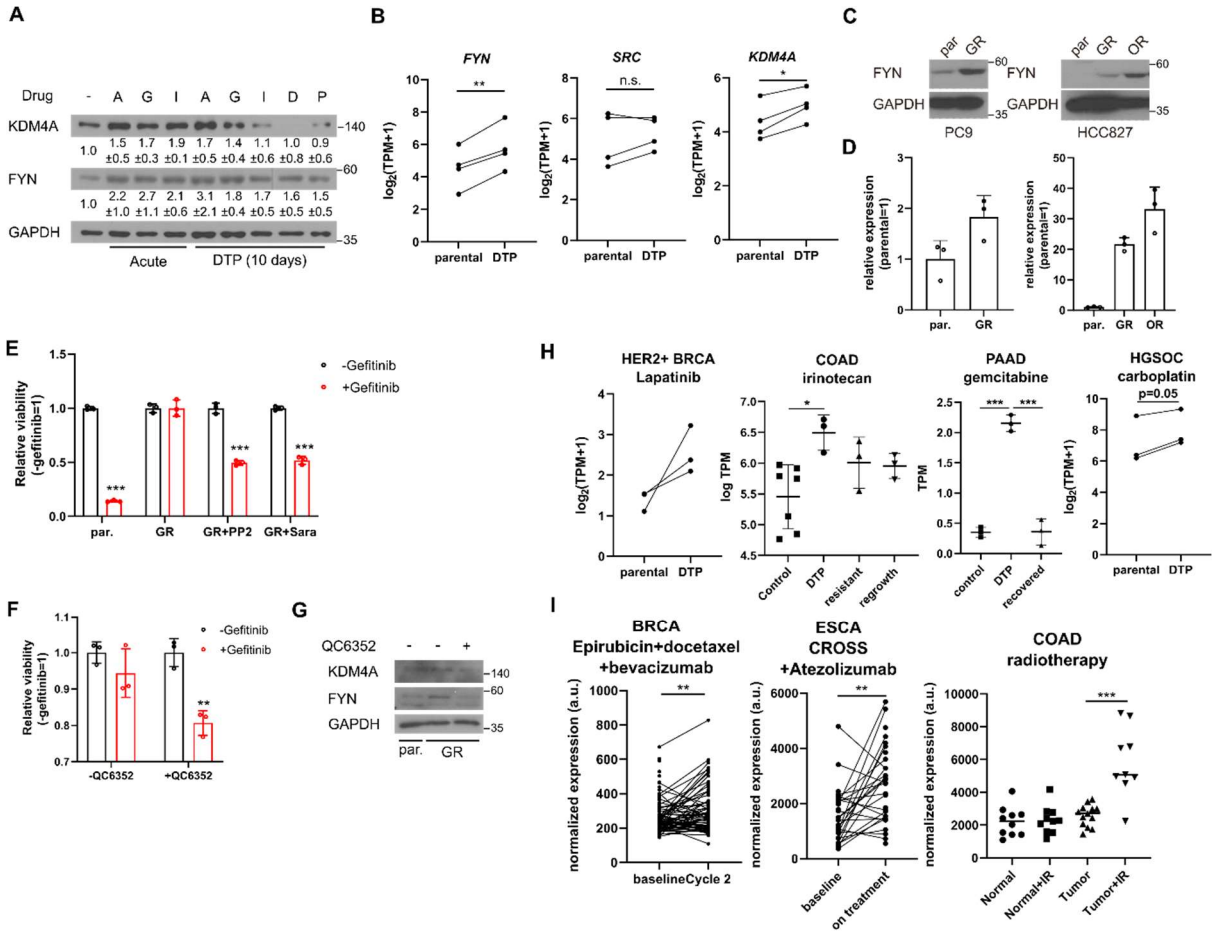

Figure 5. *FYN* and *KDM4* are associated with drug tolerance. (A) MDA-MB-231 cells treated with indicated drugs for short (acute: 2 days) and long (DTP: 10 days) time periods. A: 1μM NVP-ADW742, G: 5μM gefitinib, I: 5μM imatinib, D: 100nM doxorubicin, P: 5nM paclitaxel. Numbers below blots indicate quantification of average±s.d. expression level normalized to GAPDH in three independent experiments. (B) Summary of mRNA expressions of indicated genes in EGFR mutant lung cancer cells (parental) and their derivative osimertinib tolerant persisters (DTP). (C-D) western blots (C) and RT-qPCR (D) analyses of indicated parental and EGFR inhibitor resistant lung cancer cells. (E-F) MTT assay with PC9 parental (par.) and gefitinib resistant (GR) cells treated with indicated drug combinations (gefi: 2μM gefitinib, PP2: 5μM PP2, Sara: 5μM saracatinib, QC6352: 10μM QC6352) for 72 hours. (G) western blot analysis with PC9 cells treated with 10μM QC6352 for 48 hours. (H) *FYN* mRNA expression levels of parental and DTP populations in various cancers treated with indicated drugs.. (I) *FYN* mRNA expression levels of residual disease after indicated treatments. All data are

660 plotted as mean±s.d. Paired two-sided Student's t-test in B, H (HER2+ BRCA set and HGSOC carboplatin set),
661 and I (BRCA set and ESCA set), and unpaired two-sided Student's t-test in H (COAD and PAAD sets) and I
662 (COAD set). The expression data in B,H,I are obtained from NCBI gene expression omnibus. The accession
663 numbers of the expression data analyzed are listed in Supplementary table S2. *, $p<0.05$; **, $p<0.01$; ***,
664 $p<0.001$; n.s., $p>0.05$. All replicates are biological replicates.

665